Coupled modelling of the EBR-II SHRT-45R including photon heat deposition

COUPLED MODELLING OF THE EBR-II SHRT-45R INCLUDING PHOTON HEAT DEPOSITION

Domenico Valerio, Nicolò Abrate, Sandra Dulla,
Giuseppe Francesco Nallo and Piero Ravetto
NEMO Group, Dipartimento Energia, Politecnico di Torino
Corso Duca degli Abruzzi 24, 10129 Torino, Italy

domenico.valerio@polito.it, nicolo.abrate@polito.it, sandra.dulla@polito.it,
giuseppefrancesco.nallo@polito.it, piero.ravetto@polito.it

ABSTRACT

The Fast REactor NEutronics/Thermal-hydraulICs (FRENETIC) code has been developed during the last years at Politecnico di Torino, implementing a full-core coupled neutronic/thermal-hydraulics model for steady-state and transient analysis of liquid-metal cooled fast breeder reactor (LMFBR). In the framework of the validation activities for the code, an analysis of the sodium-cooled reactor EBR-II, previously carried out in the frame of a IAEA Coordinated Research Project, is performed with FRENETIC including the most recent physics models. In particular, photon transport and heat deposition are taken into account, a feature which has been proved in previous studies to be relevant to the correct study of the EBR-II core. To this purpose, a set of nuclear data for photons has been generated by means of the Monte Carlo code Serpent-2, and it is demonstrated that the code is able to take into account the photon heat deposition in the EBR-II.

KEYWORDS: liquid-metal-cooled fast reactor; EBR-II; multiphysics; coupled neutronics/thermal-hydraulics; gamma heat deposition

1. INTRODUCTION

Liquid-metal fast breeder rectors (LMFBRs) are innovative systems, belonging to Gen-IV reactors, that utilize liquid metal as coolant for its capability to extract great quantity of power, together with its low interaction rate with high energy neutrons, thus allowing the establishment of a fast neutron spectrum. Due to the peculiar physical phenomena characterizing these systems, the development of computational tools suitable for the design and safety analyses requires a multiphysics approach. To this aim, the Fast REactor NEutronics/Thermal-hydraulics - FRENETIC - code has been developed at Politecnico di Torino, implementing a full-core coupled neutronic/thermal-hydraulic model for LMFBR [1].

The FRENETIC code is constituted by two modules: the neutronic (NE) module solves the neutrons distribution adopting a multi-group diffusion model solved on a coarse spatial mesh, while the thermal-hydraulic (TH) module evaluates the temperature and velocity distributions using a ”quasi 3D” approach (i.e. 1D axial advection + 2D diffusion). The modules of the code have been tested in various conditions, performing also validation against experimental results [2,3]. In particular, the validation activity performed in the frame of an IAEA Coordinated Research Project (CRP) on the Experimental Breeder Reactor-II (EBR-II) has highlighted the necessity to include in the simulation capabilities of the coupled code some additional physical phenomena such as presence of the photon and decay heat source. To this aim, a new module has been added, exploiting the modelling similarities to the neutronic module, for the photon production and transport, here modelled with the same diffusive approach as for neutrons [4].

The objective of the present work is to test the capabilities of the module for photon heat deposition in the simulation of the EBR-II core, exploiting the availability of experimental and simulated data made available during the IAEA CRP activities.

2. The EBR-II reactor

The EBR-II is a sodium-cooled fast reactor designed and operated by the Argonne National Laboratory (ANL) in the years 1964-1994. An experimental program was run in the EBR-II in the years 1984-1986, named Shut-down Heat Removal Test (SHRT), to support liquid metals reactor plant design, providing test data for the validation of computation tools. The reactor was heavily instrumented to measure mass flow rates, temperatures and fission power. In particular, in the test named SHRT-45R, an unprotected transient was initiated by a loss-of-flow-accident, in order to focus the attention on the shut-down of the reactor by negative reactivity feedbacks.

The simulation activities performed during the IAEA CRP included both the characterization of the power distribution in steady-state, and the time-dependent simulation of the transients. FRENETIC was adopted to perform both validations activities [2], in absence of photon heat deposition. In this work the validation is performed again with the new capabilities of FRENETIC.

The activity is carried out in two subsequent phases. First, the nuclear data required by FRENETIC are generated by a set of Monte Carlo simulations at different temperatures using the Serpent-2 code [5] to get a temperature-dependent library for neutrons and photons. Secondly, the FRENETIC results obtained including the gamma heat deposition is accounted for are compared to the previous EBR-II results, to evaluate the role of photon heat.

3. PHOTON CONSTANT GENERATION

Since the model describing the photon propagation in a medium is the Boltzmann linear transport equation, the same homogenisation approach applied for the evaluation of neutron macroscopic cross sections can in principle be applied to gamma rays as well. For this reason, attenuation coefficients for photon must be generated, equivalent in the form of a set of neutronic cross sections for the NE module of FRENETIC. The latter uses a set of multi-group diffusion equations for the evaluation of the neutronic flux and this approach has been extended to the photonic module. However, there are some important differences between the physics of these two kind of particles. The most important is certainly the fact that photons do not only interact with the nuclei, but also with the electron cloud. Therefore, the ENDF-6 file sections devoted to photo-atomic and photo-nuclear data should be included into the ACE files employed by the Monte Carlo code to produce the homogenised and collapsed attenuation coefficient for photons. In addition to this physic, it must be also taken into account the fact that also the energy deposition mechanisms become more complex, as a portion of the energy released by fission is not deposited locally but transported by neutrons and photons [6]. This phenomenon requires that the KERMA data are included into the ACE files as well.

In order to generate a set of ACE files including all the additional data needed for the coupled neutron/photons Serpent-2 simulations, an attempt to process the latest ENDF-B/VIII release with NJOY was carried out[7]. However, at the time of the data generation, a known but not yet fixed issue in the code related to the photo-atomic data processing rendered the process unfeasible. Therefore, the nuclear data library employed for the cross section generation has been selected as the ENDF-B/VII version provided by the Serpent-2 developers team on their forum [8]. Very recently, the bug in NJOY has been fixed, therefore it will be possible in the next future to compute the multi-group constants with the ENDF-B/VIII library, thus allowing to quantify the impact of different library releases on the computed results.

In addition to the photo-atomic data generation issue, the generation procedure of the multi-group photon attenuation coefficients needed for the FRENETIC calculations has encountered various complications. Even though one of the main purposes of the Serpent-2 code is the calculation of multi-group neutron cross sections, the same default calculation methodology is not automatically applied to photon particles, thus forcing the user to set up *ad hoc* tallies in order to evaluate the reaction rates in each region and in each energy group. As a consequence, it is currently not possible to generate multi-group attenuation coefficients for photons, since Serpent-2 detectors cannot provide multi-group scattering matrices. In addition, Serpent-2 is not currently able to model also the photo-nuclear reactions, i.e. it only considers the interaction of the photons with the electron clouds. In the next future, however, the capability to model also this kind of photon reactions should become available [9], allowing a more complete simulation of photons for the FRENETIC code.

Because of the above mentioned limitations, the calculation approach adopted assumes that the photon attenuation coefficients only take into account photo-atomic interactions and are collapsed over the whole energy axis.

The last issue faced during the photon data generation process is due to the fact that, to distinguish the different photon reactions (e.g., photo-electric effect, Compton effect and pair production) a tally for each nuclide inside each region should be defined. The workaround adopted in this case is related to the structure of the EBR-II simplified model. Since the reactor is composed of homogeneous regions, the attenuation coefficient for a certain reaction x can be expressed as

$$\bar{\mu}_x = \sum_{i=1}^{N} \frac{\int dE \phi_p(E) N_i \sigma_x(E)}{\int dE \phi_p(E)}, \tag{1}$$

where the sum is performed all over the elements in each region. This means that the evaluation of each attenuation coefficient requires that only the photon flux is scored during the simulation, as the microscopic cross sections can be extracted by Serpent in an off-line calculation and then weighted on the atomic density of each element inside a specific region. Thanks to this procedure, it is possible to compute an attenuation coefficient for each separate partial reaction, allowing to gather the photo-electric effect and the pair production in a coefficient related to the absorptions and the Rayleigh and Compton scattering inside a coefficient related to the scattering. Since the FRENETIC photonic module is currently not able to model secondary photon production, the pair production is only seen as an absorption. Finally, Serpent gives values of KERMA as energy deposition in materials. Therefore, the next operation is necessary to perform the required equivalence for the diffusion model:

$$K = \frac{K_{Serpent}}{V_{Serpent}\frac{1}{E_{i+1}-E_i}\int_{E_i}^{E_{i+1}} dE\phi(E)}. \tag{2}$$

4. GENERATION OF TEMPERATURE-DEPENDENT PHOTON LIBRARIES

4.1. Reactor configuration and Serpent model

At the moment of the SHRT tests the EBR-II core was loaded with 637 elements (Fig. 1a). The reactor was radially divided into three macro regions: the inner one with a high percentage of U-235 enrichment, the second one which was the radial reflector in stainless steel and the last one for the blanket, loaded with fertile fuel. In the axial direction, each fuel assembly in the core was divided into three regions: lower reflector, active length, upper reflector. Being a breeder reactor, the slowing down of fast neutrons coming from the inner region of the reactor leads to epithermal fissions and radiative captures in the blanket, heavily loaded with fission products and U-238. The

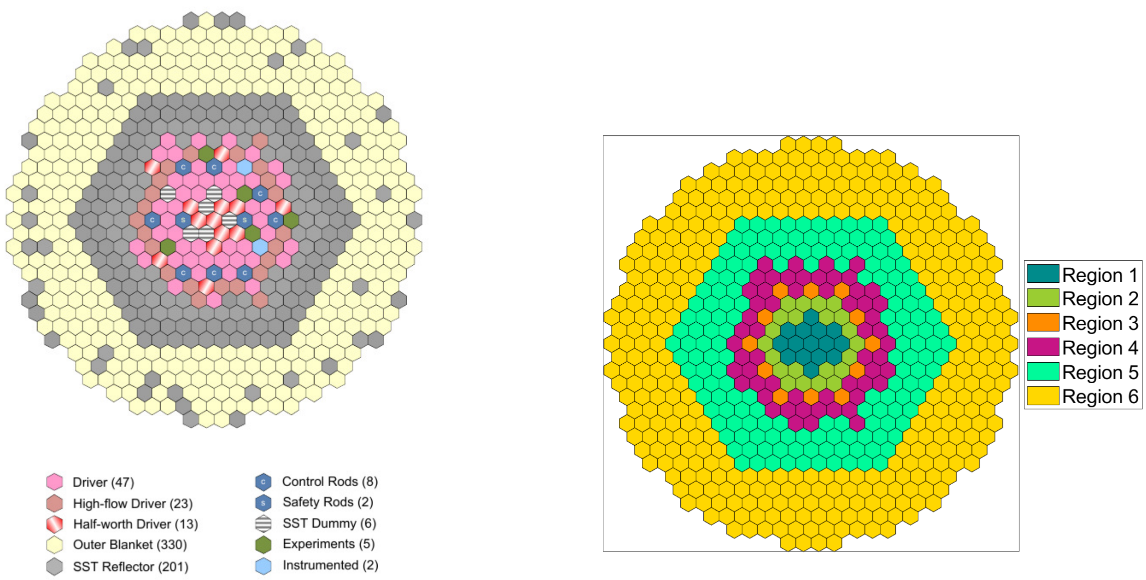

(a) Loading pattern. (b) Regions division.

Figure 1: EBR-II core loading pattern for SHRT-45R and reference Serpent model.

inner core region contained several sub-assembly types [10]: fuel driver (MARK-II AI, MARK-IIA), dummy elements (SST), control (HWC) and safety (S) rods, experimental driver (XY-16, X320C, X402A, X412, XETAGS) and instrumented ones (XX10, XX09). For the fuel assemblies, partial fuel drivers with dummy fuel pin were introduced (half-worth drivers in Fig. 1a). For the detailed geometry of each sub-assembly, please refer to [10]. The fuel composition was not fresh, therefore the isotopic composition provided must be considered for the core and the blanket. Due to the great heterogeneity in isotopic compositions and in the variety of sub-assemblies, a cylindrical spatial homogenisation has been performed to generate data for FRENETIC. A radial grouping has been performed, as reported in Fig.1b, for the Serpent simulations to partly simplify the calculation process. The volume of each region is calculated grouping the assemblies in the following way:

$$R_x = \sqrt{\frac{N \cdot A_{hex}}{\pi}}, \tag{3}$$

where N is the number of the assemblies in the considered region and A_{hex} is the area of the hexagonal sub-assembly. With this approach, the total volume and mass are preserved, since the height is the same for each fuel assemblies. In the axial direction, regions within the reflector have three subdivisions, with exception of the one which contains the HWCRs to take into account the relative position of the poison pins (which are extracted) which respect to the active length of the core. For further information, please refer to [2]. Therefore, the mesh in Serpent is composed by:

- region 1: MARK-IIAI/MARK-IIA (included those partially loaded), SR and the SST;
- region 2: MARK-IIAI/MARK-IIA, and XETAGS;
- region 3: HWCRs, XX10, XX09, XY16 and SST;
- region 4: MARK-IIA and X310C;
- region 5: reflector drivers (K);
- region 6: blanket drivers.

The Monte Carlo simulations in Serpent-2 have been performed changing the temperatures of coolant and fuel assuming that the fuel is always at a higher temperature than the coolant. This assumption is justified in the case of loss-of-flow-accident, where the thermal power decreases while the temperature of coolant increases up to the fuel temperature (at the equilibrium). The variation in temperature causes the variation in the neutron microscopic cross section and in atomic densities, therefore the libraries have been generated changing the reference value in the ENDF library according to the matrix reported in Table 1.

Table 1: Temperatures for Monte Carlo simulations in Serpent

		$T_c[K]$		
		673	973	1273
$T_f[K]$	673	x		
	973	x	x	
	1273	x	x	x

The tally [2] for the neutron cross sections has been assumed with a six groups structure (see Table 2).

Table 2: Six-group data adopted to perform the macroscopic cross sections energy collapsing and spatial homogenisation.

Group	Upper boundary [MeV]	Lower boundary [MeV]
1	$2.0 \cdot 10^{1}$	$4.0 \cdot 10^{-1}$
2	$4.0 \cdot 10^{-1}$	$6.0 \cdot 10^{-2}$
3	$6.0 \cdot 10^{-2}$	$1.0 \cdot 10^{-2}$
4	$1.0 \cdot 10^{-2}$	$1.5 \cdot 10^{-3}$
5	$1.5 \cdot 10^{-3}$	$2.5 \cdot 10^{-4}$
6	$2.5 \cdot 10^{-4}$	$1.0 \cdot 10^{-11}$

5. SELECTED SIMULATION RESULTS

It is expected that the photon energy deposition should allow for more accurately evaluating the power distribution in the core. In particular, it is no longer enforced by assumption that non-fissile assemblies have zero power deposition. In the Fig. 2, results of a preliminary steady state

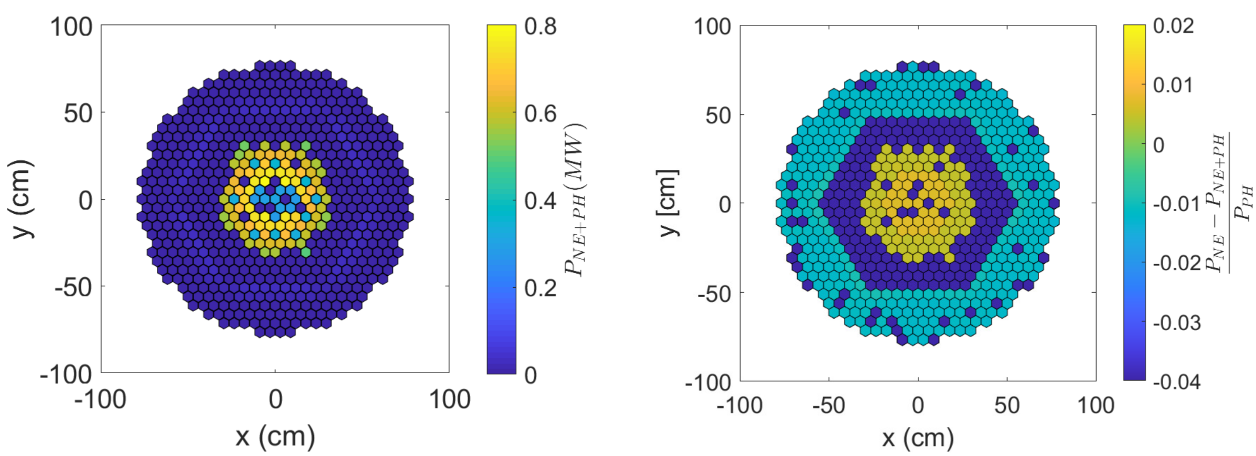

(a) Power distribution (b) Relative error

Figure 2: Radial map of the power per FA computed with (NE+PH) and without (NE) the photon transport and energy deposition model

neutronic calculation are presented. In order to take into account the thermal feedbacks in the NE module, a coupled simulation with neutron and photon diffusion together with the thermal-hydraulics module has been performed. In the Fig. 3a shows the integrated steady state thermal power deposited by photons in each of the 673 fuel assemblies of the EBR-II reactor(i.e. neutron and photon diffusion, together with thermal-hydraulics). As stated before in 3, at the moment the photo-nuclear reactions are not considered, thus γ rays due to fission and radiative capture are not taken into account for the photonic calculation performed by FRENETIC. Therefore, in the inner region of the core there is low activation and low γ production, although the dummy elements (white assemblies in Fig. 3a) are highly activated by the neutron flux. Moving to the outer regions of the core, the power deposited by photons tends to increase since the reflector is completely made by stainless steel, whereas the activation is completely damped in the blanket.

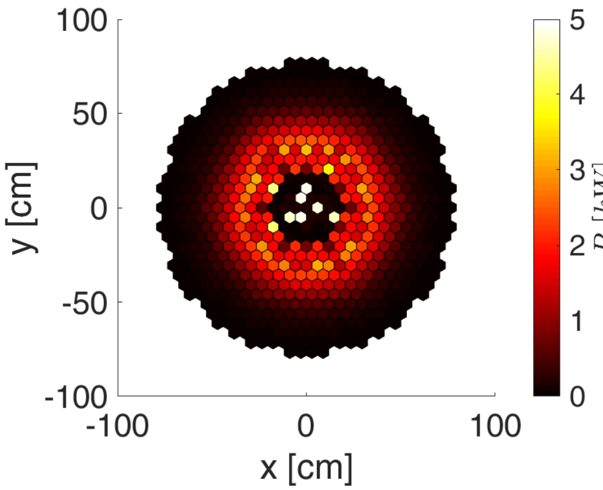

(a) Photon power map

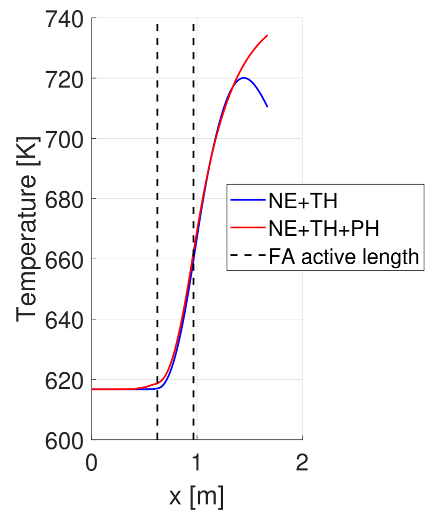

(b) XX10 temperature distributions

Figure 3: Steady state (NE+TH+PH) radial map of the photon power integrated per FA and comparison between the coolant temperature distributions calculated by FRENETIC in the experimental driver XX10.

Even if the thermal power deposited by γ rays and neutron KERMA is low with respect to the fission power, it is pivotal to state that the effect on the coolant temperature distribution is significant in those assemblies that are not loaded with fissile fuel. In particular, the experimental assembly XX10 is an instrumented driver without fissile material used during the SHRT-45R to measure the coolant temperature. In Fig. 3b a comparison in steady state between the temperature distribution of sodium is concerned. In order to show the heat exchange among the nearer assemblies, in Fig. 3b the corresponding active length of the core is reported. The blue line represents the temperature calculated when the thermal power due to photon is not considered: the region after the active length results colder since the axial reflector is not heated by gamma deposition, but only by inter-assemblies heat exchange. Conversely, the red line is the temperature of coolant when photon heat deposition is concerned: the outlet temperature is significantly increased by the γ deposition, lowering the effect of "heat sink" for the nearer assemblies. Furthermore, a slight temperature increase can be noticed in the corresponding active length.

6. CONCLUSIONS

In this paper, the FRENETIC code has been applied to simulate the gamma and neutron KERMA energy deposition in the EBR-II reactor. Nuclear data have been generated and collected in a database to be employed by the code. Computed fission and photon power deposition in steady state considering the thermal-hydraulics effects are in line with the expectations, showing how the inclusion on the heat gamma deposition has a non-negligible effect on the sodium temperature distributions. In perspective, we plan to perform the complete transient analysis of the SHRT-45R to assess the effect of photon heating. A new full-core Serpent model is foreseen, to better describe the heterogeneity of the core and related cross sections for the libraries. Furthermore, the contribution of delayed gamma emitted by the fission products will be take into account. After that, the full transient foreseen by the benchmark will be performed and the comparison against the experimental data provided for the instrumented drivers will be done.

ACKNOWLEDGEMENTS

Computational resources were provided by HPC@POLITO, a project of Academic Computing within the Department of Control and Computer Engineering at the Politecnico di Torino.

REFERENCES

[1] R. Bonifetto, S. Dulla, P. Ravetto, L. S. Richard, and R. Zanino. "A full-core coupled neutronic/thermal-hydraulic code for the modeling of lead-cooled nuclear fast reactors." *Nuclear Engineering and Design*, **volume 261**, pp. 85–94 (2013).

[2] D. Caron, R. Bonifetto, S. Dulla, V. Mascolino, P. Ravetto, D. Valerio, and R. Zanino. "Full-core coupled neutronic/thermal-hydraulic modelling of the EBR-II SHRT-45R transient." *International Journal of Energy Research*, **volume 42**, pp. 134–150 (2018).

[3] G. Nallo, N. Abrate, S. Dulla, P. Ravetto, and D. Valerio. "Neutronic benchmark of the FRENETIC code for the multiphysics analysis of lead fast reactors." *The European Physical Journal Plus*, **volume 135:238** (2020).

[4] D. Caron, S. Dulla, P. Ravetto, L. Savoldi, and R. Zanino. "Models and methods for the representation of decay and photon heat in spatial kinetics calculations." In *Proceedings of the International Conference PHYSOR 2016*, pp. 2416–2425. Sun Valley, ID (2016).

[5] J. Leppänen, M. Pusa, T. Viitanen, V. Valtavirta, and T. Kaltiaisenaho. "The Serpent Monte Carlo code: Status, development and applications in 2013." *Annals of Nuclear Energy*, **volume 82**, pp. 142 – 150 (2015).

[6] R. Tuominen, V. Valtavirta, and J. Leppänen. "New energy deposition treatment in the Serpent 2 Monte Carlo transport code." *Annals of Nuclear Energy*, **volume 129**, pp. 224–232 (2019).

[7] R. E. Macfarlane, C. Authors, D. W. Muir, R. M. Boicourt, A. C. Kahler, J. L. Conlin, and W. Haeck. "The NJOY Nuclear Data Processing System, Version 2016." Technical report (2018).

[8] "Discussion forum for Serpent users." (2020). URL https://ttuki.vtt.fi/serpent/.

[9] T. Kaltiaisenaho. "Photonuclear Reactions in Serpent 2 Monte Carlo Code." In *Proceedings of the ANS International Conference M&C2019*. Portland, OR (2019).

[10] T. Fei, A. Mohamed, and T. K. Kim. "Neutronic benchmark specifications for EBR-II Shutdown Heat Removal Test SHRT-45R - Revision 1." Technical report, Argonne National Laboratory (2013).